J Supercond Nov Magn (2011) 24: 1201–1205
DOI 10.1007/s10948-010-1110-4

ORIGINAL PAPER

On the Structural Transition Driven by Band Nesting in 1111 Pnictides

Alessandro Ricci · Nicola Poccia · Boby Joseph · Antonio Bianconi

Received: 10 December 2010 / Accepted: 12 December 2010 / Published online: 5 January 2011

Abstract The lattice critical response in REFeAsO (RE = Pr, Nd and Sm) oxypnictides near the orthorhombic-to-tetrahedral structural phase transition is studied using ultra-high-resolution X-ray diffraction in the temperature range 4 to 250 K. The critical exponent of the structural phase transition β is found to decrease with decreasing RE size. The β values determined to be 0.212, 0.209 and 0.194, respectively, for PrOFeAs, NdOFeAs and SmOFeAs. Temperature hysteresis is observed for all the REFeAsO, with ΔT being of the order of 2 to 3 K. The results are discussed in the frame of Fermi surface nesting induced structural transition in the pnictides.

Keywords High-temperature superconductivity · Pnictides · Structural phase transition · Powder diffraction

1 Introduction

The recent discovery of high-temperature superconductivity (HTS) in the iron pnictides [1] has provided a new class of materials for the search of the physical mechanism that allows a quantum coherent condensate to avoid the effects of temperature decoherence. The discovery of HTS in $LaO_{1-x}FeAsF_x$ was soon followed by the discovery of a different class of superconducting iron-based compounds, among which the quaternary systems "1111" [2, 3] (REFeAsO, RE stands for rare earth) and ternary "122" (AFe_2As_2, A stands for Ba, Ca, Sr, etc.) systems are the most investigated. Superconductivity arises in the 1111 systems by the partial fluorine substitution for the oxygen [1], or by the creation oxygen defects [2]. On the other hand, substitution of Fe by K, Ni, etc. is found to result in the superconducting transition in the 122 systems. Interestingly, in both cases, the bulk superconductivity appears by the suppression of the long-range magnetic ordering of the parent compounds. But in several cases complete suppression of the magnetic ordering is not necessary for the appearance of superconductivity (SC) and we have co-existing magnetism and superconductivity. The parent compounds, which do not show the SC, show a structural transition from the room temperature tetragonal to orthorhombic structure [4–8]. In the 1111 system, the structural and magnetic transitions do not coincide, whereas the structural and magnetic transitions coincide in the 122 systems. There are several reports available on the structural phase transition in these systems, however, several open questions still remain. For example, consensus has not been reached on the order of the phase transition and its implications. Superconductivity has been induced by oxygen defects in the fluorite spacers in iron-based oxypnictides Sm[O1 − x]FeAs, Nd[O1 − x]FeAs and Pr[O1 − x]-FeAs with the maximum critical temperature being 43, 51.9 and 52 K, respectively [2]. Oxygen defects induce electron doping of the Fe derived bands crossing the Fermi level and the electronic/magnetic structure is very sensitive to different atomic substitutions and rare-earth (RE) ions [9–12]. The change of the RE atomic radius induces a change of the elastic misfit strain between the superconducting Fe layers and the intercalated layers [13, 14], like in cuprates, and diborides [15–17]. The multi-layer architecture, a common feature of cuprates, diborides and pnictides, underlines the relevance of lattice effects for high-temperature superconductivity. The structure of the iron pnictide superconductors is made of a superlattice of $[FeAs]_{\infty}^{-Q+\delta}$ with $Q = 1$, layers

A. Ricci (✉) · N. Poccia · B. Joseph · A. Bianconi
Department of Physics, Sapienza University of Rome,
P. le A. Moro 2, 00185 Rome, Italy
e-mail: alessandro.ricci@uniroma1.it

intercalated by spacers (oxide layers like $[LnF_yO_{1-y}]_{\infty}^{+Q-\delta}$ or $[LnFO_{1-y}]_{\infty}^{+Q-\delta}$ in the "1111" family or metallic atomic layers $[(A_{1-x}^{+2}B_x^{+1})_{1/2}]_{\infty}^{+Q-\delta}$ in the "122" family, and therefore they represent practical realizations of a 'heterostructure at the atomic limit (HsAL)' that was described to be the essential material architecture for the emergence of HTS [18]. All of them contain a characteristic layer of FeAs layers made of a tetrahedral network (with As atoms located at the apical sites of the tetrahedron) corresponding to the featured planar CuO_2 plane in cuprates and honey-comb 2D lattice of boron in diborides. These results have recently been applied to design a new heterostructure at the atomic limit for functional materials [19]. In pnictides, EXAFS and XANES [20–24] measurements have shown the local lattice fluctuations like in cuprates [25].

It has been found that the Fe–As bond length hardly shows any change, suggesting the strongly covalent nature of this bond, while the Fe–Fe and Fe–Re bond lengths decrease with decreasing rare-earth size. In support of the important role played by the local structure, transmission electron microscopy (TEM) showed in REFeMO (R = La, Nd; M = As, P) materials complex structural transitions in both crystalline symmetry and local microstructural features [26]. The crystalline structural order has been studied in pnictides by high-resolution synchrotron X-ray diffraction measurements on powder samples of REFeAsO (Re = Pr, Nd, Sm) synthesized by conventional solid-state reaction method [2]. The structural instability due to the proximity to a structural phase transition is accompanied by a magnetic instability as reported in $Sm[O_{1-x}F_x]FeAs$ by several transport properties measurements, in NdOFeAs and PrOFeAs by polarized and unpolarized neutron diffraction. In SmOFeAs, NdOFeAs and PrOFeAs the tetragonal–orthorhombic phase transition is found on cooling below 135, 136 and 150 K, respectively [27–29]. This transition precedes magnetic ordering in the parent R-1111 compounds, whereas both transitions occur simultaneously in AFe_2As_2. However, still we need more experiments on single crystals and powders using the same experimental setup for a more complete picture on the issue and the discussion is still open.

2 Results

Here we report a systematic high-resolution synchrotron X-ray diffraction study on the structural phase transition in 1111 pnictides samples using the parent compounds based on Pr, Nd and Sm. The order parameter, β, describing the power-law divergence measured for the above three 1111 systems, shows an interesting rare-earth size dependence. β is found to increase with decreasing rare-earth size.

The samples were contained in a 0.5 mm diameter silica capillaries. The high-resolution synchronous X-ray diffraction measurements were made at the powder diffraction beamline X04SA of the SLS facility at Paul Scherrer Institute (PSI), Villigen, Zurich. The angular acceptance of the beamline is 0.23 mrad vertical by 2.5 mrad horizontal. In the monochromatic mode, the energy resolution is determined by the Si 111 monochromating crystals to be 0.014%. A helium cryostat allows us to study a range of temperature from 4 K to room temperature. High angular and temperature (0.5 K) resolution allows a good estimate of the critical exponents of order parameters of these systems.

Data analysis was performed with the GSAS suite of Rietveld analysis programs. All systems at room temperature has a tetragonal structure (T) and their unit cell belongs to space group P4/nmm [2, 3, 14]. With decreasing temperature, as already noted, these systems show a structural transition, and their unit cell becomes orthorhombic (O) with space group Cmma. Many high-resolved profiles have been collected at numerous temperatures between 300 and 4 K over a shorter angular range (2θ between 1° and 50° with a wavelength of 0.495926 Å. Ultra-high-resolution X-ray diffraction allows us to better evaluate the structural transition temperature (T_s) in different samples. The peak $(220)_T$ of the tetragonal structure splits below T_s, into the $(400)_O$ and $(040)_O$ reflections of the Cmma orthorhombic phase. Three 3D color plots of the structural transition for the Pr, Nd and Sm parent compound samples have been reported in Fig. 1.

Figure 2 shows the evolution of the crystallographic axes a and b as a function of temperature for the 1111 systems. We agree with previous studies but compared with those earlier reports, the high angular and temperature (0.5 K) resolution used in the present study allows a better estimate of the critical exponents of order parameters of these systems. The structural phase transition temperatures observed in the present measurements are 150, 145 and 133 K, respectively, for the PrOFeAs, NdOFeAs and SmOFeAs samples (Fig. 2).

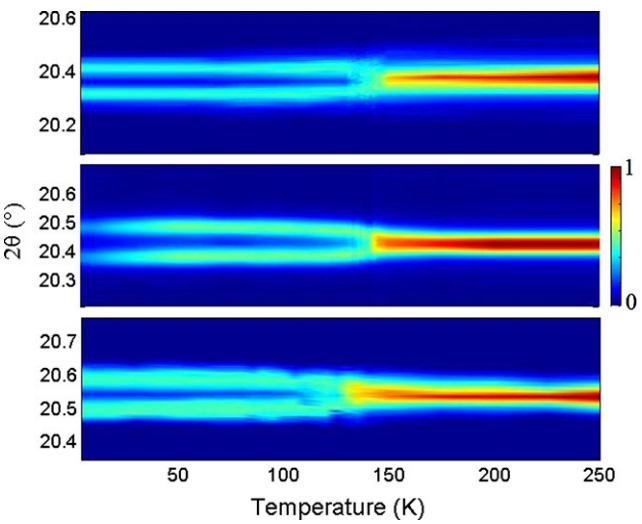

Fig. 1 3D color plots of the structural transition for the Pr *(upper panel)* Nd (*center panel*) and Sm (*bottom panel*) parent compounds

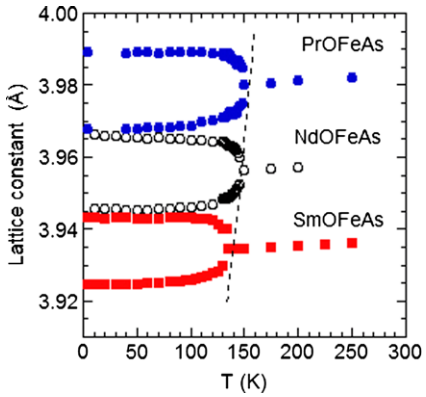

Fig. 2 The lattice constant a (b) as a function of temperature T(K). The figure shows the characteristic structural phase transition from tetragonal (P4/nmm) to orthorhombic (Cmma) symmetry of 1111 pnictides. The a and b lattice parameters are divided by $\sqrt{2}$ at a temperature below the transition, T_s. *Error bars* are smaller than the size of the symbols

The order parameter of the structural transition (OP) is calculated by the formula $OP = [(a - b)/(a + b)] \cdot 10^3$ where a and b are the lattice parameters of unit cell.

The critical temperature T_s measured in the warming cycle are 153, 148 and 135 K for systems containing Re = Pr, Nd and Sm. This result measured in the same experimental run confirms that for this set of samples the critical temperature T_s decreases by decreasing the ionic radius of the rare-earth ions in the spacer layers: 113 pm for Pr^{3+}112.3 pm for Nd^{3+} and 109.8 pm for Sm^{3+}.

Figure 3 shows the comparison of the OP between the cooling cycle and the heating one. From the figure the presence of a small hysteresis is evident between the heating and cooling cycle. The magnitude of this hysteresis is about $\Delta T = 3 \pm 1$ K for PrOFeAs and NdOFeAs and while $\Delta T 2 \pm 1$ K for SmOFeAs. It is to be noted that the temperature during the measurements was controlled with an accuracy much better than 0.5 K.

In Fig. 4 we have plotted the OP as a function of reduced temperature, obtained by dividing the temperature for the T_s of each samples. We fit the data to a simple power-law, $(1 - T/T_s)^{\beta}$, in order to obtain the critical exponent $\tilde{\beta}$. The β coefficient is 0.212 for PrOFeAs 0.209 for NdOFeAs and 0.194 for the parent compound containing Sm. These results show that the critical exponent β decreases with decreasing size of the rare earth (with increasing atomic number Z). These values are consistent with that found for LaOFeAs, which happens to be 0.22(6), a value greater than any found for pnictides [30, 31]. This confirms the upward trend of β coefficient increases the size of rare earth. The values found in this work confirm a substantial difference in the structural phase transition behavior of 1111 and 122 family of pnictides. In the latter, in fact, the critical exponent of structural transition OP is 0.988(1) for $SrFe_2As_2$, 0.112(1) for EuFe2As2 and about 0.125(6) for Ba A-122

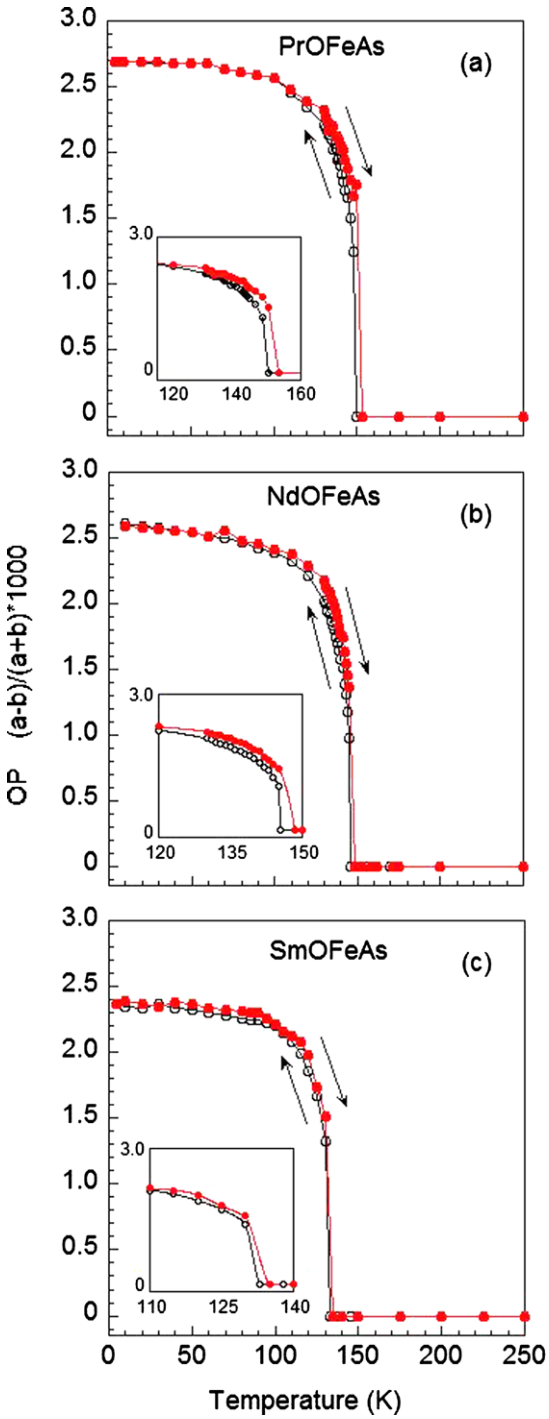

Fig. 3 Plot showing comparison of the structural order parameter $OP = (a - b)/(a + b) \cdot 10^3$ in cooling (*open dots*) and in warming (*fill dots*) cycle. *Error bars* are within data points (1 K). The figure shows a small hysteresis of 3 K for both systems PrOFeAs (panel **a**) and NdOFeAs (panel **b**) and 2 K for the SmOFeAs (panel c). The inset shows the $(200)_T$ Bragg reflection in the cycle of cooling (*black empty circle*) and the splitted $(200)_T$ in warming cycle (*red filled circle*) at the same transition temperature

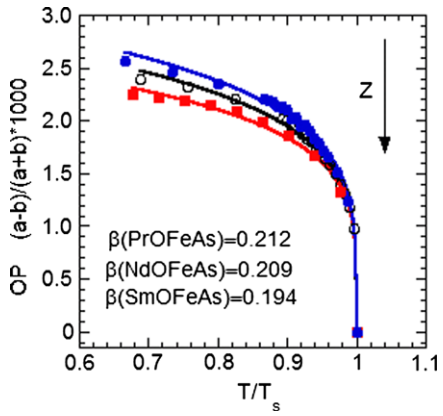

Fig. 4 Plots of the FWHM as a function of reduced temperature T/T_S on warming (*red solid line*) and cooling (*blue solid line*) for (**a**) PrOFeAs, (**b**) NdOFeAs and SmOFeAs

compound, which are not too far from 1/8, which is the expected value for a 2D-Ising model [32]. In contrast to measurements made by neutron diffraction [27], the splitting of the peak $(200)_T$ can be resolved in two distinct peaks due to ultra-high 2θ resolution. This allows for better evaluation of the order parameter exponent β of the structural transition and for resolving the hysteresis loop. The close dependence of the β coefficient on rare-earth size emphasizes the important role of another variable, besides doping, to describe the phase diagram of HTS pnictides like in cuprates and diborides [14].

3 Conclusions

From the comparison of 1111 and 122 families, it is clear that the two families have different Fermi surface nesting. The results of the present experiments further reveal that also the β exponents of structural phase transition are different. In addition, the two families show distinct behavior of the structural phase transition, with 1111 revealing the structural phase transition to occur at different temperature than the one for the spin ordering, unlike the 122 system, in which the two temperatures coincide suggesting stronger nesting for the 122. Apart from the above, the present results clearly show a temperature hysteresis, albeit small, in the 1111 system, while the hysteresis in the 122 is controversial. In any case, the observed temperature hysteresis and higher superconducting critical temperature in the 1111 suggests important role of correlation between the structural transition and the Fermi surface nesting.

Here it is worth discussing the recent STM/STS experiments on the Fe-pnictides showing nanostructures of dimensions about eight times the Fe–Fe distance, aligned along the crystal a axis [33]. Indeed, the one-dimensional electronic band structure reveals that the bottom of the band appears not far from the Fermi level. This is clear evidence for the proximity to an electronic topological transition (ETT), similar to the cases of other HTS layered materials, in which the superconductivity appears while the chemical potential is tuned near an ETT [34–37]. In the proximity of an ETT a Feshbach resonance (or shape resonance) of the exchange-like interband pairing is switched on and the quantum condensates become protected by the decoherence effects of high temperature [38] as well as has been proposed for biological systems [39]. In this scenario, the physical system is in a state with structural instability with granular [40, 41], scale-free [42] and multigap superconductivity [43–45]. We have studied the structural phase transition in the REFeAsO oxypnictides using high-resolution X-ray powder diffraction. The critical exponent of the structural phase transition order parameter β is found to show a systematic rare-earth size dependence with the critical values of about 0.2, expected for a two-dimensional Ising model. Precise control over the sample temperature permitted us to reveal a temperature hysteresis of about 3 ± 1 K for all the samples. Comparing the present findings to the 122 system, we have argued that the two systems have a different character of structural phase transition, derived by a different Fermi surface nesting. The results are consistent with an important role of the Fermi surface derived structural phase instability in a multiband superconductor with chemical potential tuned near an electronic topological transition (ETT).

Acknowledgements We are grateful to Z.-A. Ren and Z.-X. Zhao for providing the powder 1111 samples and Naurang L. Saini for helpful suggestions. This project has been supported by Sapienza University of Rome research funding, and we thank the help of the staff of diffraction beamline X04SA of the SLS facility and the Paul Scherrer Institute (PSI), Villigen, Zurich, for support of European researchers.

References

1. Kamihara, Y., Watanabe, T., Hirano, M., Hosono, H.: J. Am. Chem. Soc. **130**, 3296 (2008). http://dx.doi.org/10.1021/ja800073m
2. Ren, Z.-A., Zhao, Z.-X.: Adv. Mater. **21**, 4584 (2009). http:dx.doi.org/10.1002/adma.200901049
3. Ivanovskii, A.L.: Phys. Usp. **51**, 1229 (2008). http://dx.doi.org/10.1070/PU2008v051n12ABEH006703
4. Nomura, T., Kim, S.W., Kamihara, Y., Hirano, M., Sushko, P.V., Kato, K., Takata, M., Shluger, A.L., Hosono, H.: Supercond. Sci. Technol. **21**, 125028+ (2008). http://dx.doi.org/10.1088/0953-2048/21/12/125028
5. McGuire, M.A., Hermann, R.P., Sefat, A.S., Sales, B.C., Jin, R., Mandrus, D., Grandjean, F., Long, G.J.: New J. Phys. **11**, 025011+ (2009). http://dx.doi.org/10.1088/1367-2630/11/2/025011
6. Fratini, M., Caivano, R., Puri, A., Ricci, A., Ren, Z.-A., Dong, X.-L., Yang, J., Lu, W., Zhao, Z.-X., Barba, L., et al.: Supercond. Sci. Technol. **21**, 092002+ (2008). http://dx.doi.org/10.1088/0953-2048/21/9/092002
7. Martinelli, A., Palenzona, A., Ferdeghini, C., Putti, M., Emerich, H.: J. Alloys Compd. **477**, L21 (2009). http://dx.doi.org/10.1016/j.jallcom.2008.10.153

8. Ricci, A., Fratini, M., Bianconi, A.: J. Supercond. Nov. Magn. **22**, 305 (2009). http://dx.doi.org/10.1007/s10948-008-0434-9
9. Lebegue, S., Yin, Z.P., Pickett, W.E.: New J. Phys. **11**, 025004+ (2009). http://dx.doi.org/10.1088/1367-2630/11/2/025004
10. Medici, L., Hassan, S.R., Capone, M.: J. Supercond. Nov. Magn. **22**, 535 (2010). http://dx.doi.org/10.1007/s10948-009-0458-9
11. Kamihara, Y., et al.: Preprint. arXiv:0904.3173v2 [cond-mat.supr-con] (2009)
12. Jeglič, P., Bos, J.W.G., Zorko, A., Brunelli, M., Koch, K., Rosner, H., Margadonna, S., Arčon, D.: Phys. Rev. B **79**, 094515+ (2009). http://dx.doi.org/10.1103/PhysRevB.79.094515
13. Ricci, A., Poccia, N., Ciasca, G., Fratini, M., Bianconi, A.: J. Supercond. Nov. Magn. **22**, 589 (2009). http://dx.doi.org/10.1007/s10948-009-0473-x
14. Ricci, A., Poccia, N., Joseph, B., Barba, L., Arrighetti, G., Ciasca, G., Yan, J.Q., McCallum, R.W., Lograsso, T.A., Zhigadlo, N.D., et al.: Phys. Rev. B **82**, 144507+ (2010). http://dx.doi.org/10.1103/PhysRevB.82.144507
15. Fratini, M., Poccia, N., Bianconi, A.: J. Phys. Conf. Ser. **108**, 012036+ (2008). http:dx.doi.org/10.1088/1742-6596/108/1/012036
16. Bianconi, A., Agrestini, S., Bianconi, G., Di Castro, D., Saini, N.L.: J. Alloys Compd. **537**, 317–318 (2001). http://dx.doi.org/10.1016/S0925-8388(00)01383-9
17. Poccia, N., Fratini, M.: J. Supercond. Nov. Magn. **22**, 299–303 (2009). http://dx.doi.org/10.1007/s10948-008-0435-8
18. Bianconi, A.: USA Patent, Patent number: 6265019 U.S. Classification 427/62; 505/121 International Classification H01L 3912 Process of increasing the critical temperature Tc of a bulk superconductor. http://www.google.com/patents/about?id=WJcHAAAAEBAJ&dq=bianconi+superconductor
19. Ricci, A., Joseph, B., Poccia, N., Xu, W., Chen, D., Chu, W.S., Wu, Z.Y., Marcelli, A., Saini, N.L., Bianconi, A.: Supercond. Sci. Technol. **23**, 052003+ (2010). http://dx.doi.org/10.1088/0953-2048/23/5/052003
20. Iadecola, A., Agrestini, S., Filippi, M., Simonelli, L., Fratini, M., Joseph, B., Mahajan, D., Saini, N.L.: Europhys. Lett. **87**, 26005 (2009). http://dx.doi.org/10.1209/0295-5075/87/26005
21. Joseph, B., Iadecola, A., Fratini, M., Bianconi, A., Marcelli, A., Saini, N.L.: J. Phys., Condens. Matter **21**, 432201+ (2009). http://dx.doi.org/10.1088/0953-8984/21/43/432201
22. Mustre de León, J., Lezama-Pacheco, J., Bianconi, A., Saini, N.L.: J. Supercond. Nov. Magn. **22**, 579 (2009). http://dx.doi.org/10.1007/s10948-009-0461-1
23. Kroll, T., et al.: Phys. Rev. B **78**, 220502+ (2008). http://dx.doi.org/10.1103/PhysRevB.78.220502
24. Kurmaev, E.Z., et al.: Phys. Rev. B **78**, 220503+ (2008). http://dx.doi.org/10.1103/PhysRevB.78.220503
25. Bianconi, A., Saini, N.L., Lanzara, A., Missori, M., Rossetti, T., Oyanagi, H., Yamaguchi, H., Oka, K., Ito, T.: Phys. Rev. Lett. **76**, 3412 (1996). http://dx.doi.org/10.1103/PhysRevLett.76.3412
26. Ma, C., Zeng, L.J., Yang, H.X., Shi, H.L., Che, R.C., Liang, C.Y., Qin, Y.B., Chen, G.F., Ren, Z.A., Li, J.Q.: Europhys. Lett. **84**, 47002+ (2008). http://dx.doi.org/10.1209/0295-5075/84/47002
27. McGuire, M.A., Christianson, A.D., Sefat, A.S., Sales, B.C., Lumsden, M.D., Payzant, E.A., Mandrus, D., Luan, Y., Keppens, V., et al.: Phys. Rev. B **78**, 094517+ (2008). http://dx.doi.org/10.1103/PhysRevB.78.094517
28. Tropeano, M., Fanciulli, C., Ferdeghini, C., Marre, D., Siri, A.S., Putti, M., Martinelli, A., Ferretti, M., Palenzona, A., Cimberle, M.R., et al.: Supercond. Sci. Technol. **22**, 034004+ (2009). http://dx.doi.org/10.1088/0953-2048/22/3/034004
29. Chen, Y., Lynn, J.W., Li, J., Li, G., Chen, F., Luo, J.L., Wang, N.L., Dai, P., Cruz, C.D., Mook, H.A.: Phys. Rev. B **78**, 064515+ (2008). http://dx.doi.org/10.1103/PhysRevB.78.064515
30. Wilson, S.D., Yamani, Z., Rotundu, C.R., Freelon, B., Courchesne, E.B., Birgeneau, R.J.: Phys. Rev. B **79**, 184519+ (2009). http://dx.doi.org/10.1103/PhysRevB.79.184519
31. Wilson, S.D., Rotundu, C.R., Yamani, Z., Valdivia, P.N., Freelon, B., Bourret-Courchesne, E., Birgeneau, R.J.: Preprint. arXiv:0910.0489v1 [cond-mat.supr-con] (2009)
32. Tegel, M., Rotter, M., Weiss, V., Schappacher, F.M., Pottgen, R., Johrendt, D.: J. Phys., Condens. Matter **20**, 452201+ (2008). http://dx.doi.org/10.1088/0953-8984/20/45/452201
33. Chuang, T.M., Allan, M.P., Lee, J., Xie, Y., Ni, N., Bud'ko, S.L., Boebinger, G.S., Canfield, P.C., Davis, J.C.: Science **327**, 181 (2010). http://dx.doi.org/10.1126/science.1181083
34. Kugel, K.I., Rakhmanov, A.L., Sboychakov, A.O., Poccia, N., Bianconi, A.: Phys. Rev. B **78**, 165124+ (2008). http://dx.doi.org/10.1103/PhysRevB.78.165124
35. Kugel, K.I., Rakhmanov, A.L., Sboychakov, A.O., Kusmartsev, F.V., Poccia, N., Bianconi, A.: Supercond. Sci. Technol. **22**, 014007+ (2009). http://dx.doi.org/10.1088/0953-2048/22/1/014007
36. Innocenti, D., Poccia, N., Ricci, A., Valletta, A., Caprara, S., Perali, A., Bianconi, A.: Phys. Rev. B **82**, 184528+ (2010). http://dx.doi.org/10.1103/PhysRevB.82.184528
37. Innocenti, D., Caprara, S., Poccia, N., Ricci, A., Valletta, A., Bianconi, A.: Supercond. Sci. Technol. **24**, 015012+ (2011). http://dx.doi.org/10.1088/0953-2048/24/1/015012
38. Caivano, R., Fratini, M., Poccia, N., Ricci, A., Puri, A., Ren, Z.-A., Dong, X.-L., Yang, J., Lu, W., Zhao, Z.-X., et al.: Supercond. Sci. Technol. **22**, 014004+ (2009). http://dx.doi.org/10.1088/0953-2048/22/1/014004
39. Poccia, N., Ricci, A., Innocenti, D., Bianconi, A.: Int. J. Mol. Sci. **10**, 2084–2106 (2009). http://dx.doi.org/10.3390/ijms10052084
40. Zola, D., Polichetti, M., Adesso, M.G., Fittipaldi, R., Cirillo, C., Luo, J., Chen, G.F., Li, Z., Wang, N.L., Vecchione, A., et al.: J. Supercond. Nov. Magn. **22**, 609 (2009). http://dx.doi.org/10.1007/s10948-009-0477-6
41. Di Gioacchino, D., Marcelli, A., Zhang, S., Fratini, M., Poccia, N., Ricci, A., Bianconi, A.: J. Supercond. Nov. Magn. **22**, 549 (2009). http://dx.doi.org/10.1007/s10948-009-0470-0
42. Daghero, D., Tortello, M., Gonnelli, R.S., Stepanov, V.A., Zhigadlo, N.D., Karpinski, J.: J. Supercond. Nov. Magn. **22**, 543. http://dx.doi.org/10.1007/s10948-009-0480-y
43. Fratini, M., Poccia, N., Ricci, A., Campi, G., Burghammer, M., Aeppli, G., Bianconi, A.: Nature **466**, 841 (2010). http://dx.doi.org/10.1038/nature09260
44. Rodríguez-Núñez, J.J., Schmidt, A.A., Citro, R., Noce, C.: J. Supercond. Nov. Magn. **22**, 539 (2009). http://dx.doi.org/10.1007/s10948-009-0466-9
45. Bianconi, A., Valletta, A., Perali, A., Saini, N.L.: Physica C, Supercond. **296**, 269 (1998). http://dx.doi.org/10.1016/S0921-4534(97)01825-X